ISSN (Print) 1226-1750
ISSN (Online) 2233-6656
Journal of Magnetics 22(2), 333-343 (2017) https://doi.org/10.4283/JMAG.2017.22.2.333

Skin Effect of Rotating Magnetic Fields in Liquid Bridge

Yi Zhang[1,2,4], Zhong Zeng[1,2,3]*, Liping Yao[1,5], Yuui Yokota[6], Yoshi Kawazoe[7], and Akira Yoshikawa[6]

[1]*State Key Laboratory of Coal Mine Disaster Dynamics and Control (Chongqing University), P.R. China*
[2]*Department of Engineering Mechanics, Chongqing University, Chongqing 400044, P.R. China*
[3]*State Key Laboratory of Crystal Material (Shandong University), P.R. China*
[4]*Chongqing Key Laboratory of Heterogeneous Material Mechanics (Chongqing University), P.R. China*
[5]*College of Engineering and Technology, Southwest University, Chongqing 400716, P.R. China*
[6]*Institute for Materials Research, Tohoku University, Sendai 980-8577, Japan*
[7]*New Industry Creation Hatchery Center, Tohoku University, Sendai 980-8579, Japan*

(Received 2 February 2016, Received in final form 20 April 2017, Accepted 21 April 2017)

A rotating magnetic field (RMF) Φ_1-Φ_2 model was developed in consideration of the skin effect. The rotating magnetic field's induced three-dimensional flow was simulated numerically, and the influence of the skin effect was investigated. The rotating magnetic field drives the rotating convection in the azimuthal direction, and a secondary convection appears in the radial-meridional direction. The results indicate that ignoring the skin effect results in a smaller azimuthal velocity component and larger radial and axial velocity components, and that the deviation becomes more obvious with the larger dimensionless shielding parameter *K*.

Keywords : Rotating magnetic Fields, Computer simulation, Fluid flows, Skin effect, Φ_1-Φ_2 model

1. Introduction

With the rapid development of information technology, there has been a growing demand for large and high-quality semiconductor single crystals. During crystal growth, the heat and mass transfer of melt play important roles in determining crystal quality. In particular, for large crystals, convection control becomes significant to the achievement of high quality. Nowadays, the magnetic field, either static [1, 2] or rotating, is essential to the control of melt convection. However, a rotating magnetic field, relative to a static one, requires much less energy, and therefore attracts increasing attention in the research field [3-8].

In a rotating magnetic field, the skin effect leads to a non-uniform magnetic field in melt and depends on the shielding parameter, $K = \sigma\mu\omega R^2$ (where σ is the electrical conductivity, μ is the magnetic permeability, ω is the rotating angular frequency, and R is the radius of melt). The shielding parameter, K, is usually used to characterize the interaction between the magnetic field and the electrically conducting melt. The condition $K \ll 1$ means that the magnetic field distribution is almost completely unaffected by the conducting melt; in other words, the rotating magnetic field is taken to penetrate into the melt volume without any change, under which condition the skin effect is negligible. In most of the research on the rotating magnetic field for convection control in crystal growth, the dimensionless shielding parameter K is assumed to be $K \ll 1$ [3-8]. Nevertheless, in more typical cases, K is expected to be larger than 1, which indicates that the magnetic field is reduced when penetrating into the melt, because the magnetic field lines are expelled due to the high conductivity of the melt and the large angular frequency of the magnetic field. In the growth of large-size crystals, the dimensionless shielding parameter K can be large, for example, 8.88 for a rotating magnetic field of 50 Hz frequency in a silicon melt of 15 cm radius. In this case, the skin effect of the rotating magnetic field should be studied.

The skin effect in the rotating magnetic field has been investigated in [9-14]. E. Dahlberg [9] reported the expression of the Lorentz force with the skin effect by ignoring the effects of the convection on the electric current and the magnetic field. Volz and Mazuruk [11] theoretically studied the Lorentz force in melt within a

*Corresponding author: Tel: +86 13638333680
Fax: +86 23 65111067, e-mail: zzeng@cqu.edu.cn

finite-length cylinder under a rotating magnetic field, and obtained an approximate solution of the azimuthal Lorentz force by ignoring the interaction between the field and the melt convection. Spitzer *et al.* [12, 13] presented approximate expressions of Lorentz force (in the radial and azimuthal directions) in Czochralski crystal growth while the effects of convection on the electric current and magnetic field were ignored. In all of the above investigations, the infinite model was adopted to calculate the distribution of the magnetic field. Moreover, in order to derive the Lorentz force, the following assumptions were taken into account: the height of the melt is infinite; the contribution of melt convection to the Lorentz force is negligible, and only the azimuthal Lorentz force is derived. However, Yao *et al.* [8] stated that the over-simplified RMF infinite model might lead to large deviations in convection structure and temperature distribution, because the components of the Lorentz force in both the radial and axial directions can affect the melt flow.

In the present study, in calculating the distribution of the magnetic field, the assumption of an infinite-length inductor of cylindrical symmetry was taken, as in the preceding reports, but in subsequently deriving the Lorentz force, all of the other above-noted assumptions were abandoned. The rotating magnetic field Φ_1-Φ_2 model, including all of the components of the Lorentz force, was derived, and the interaction between the melt convection and the magnetic field was considered in the developed rotating magnetic field Φ_1-Φ_2 model. Then, the skin effect of the rotating magnetic field was investigated via a three-dimensional flow driven by that field.

2. Physical and Mathematical Model

The geometrical model, as exhibited in Fig. 1, is a cylindrical liquid bridge suspended between two disks. The rotating magnetic field with strength B_0 rotates with angular frequency ω in the azimuthal direction, and the convection is driven by the rotating magnetic field due to the Lorentz force. The height and radius of the liquid bridge are H and R, respectively. Basically, both the magnetic strength and the gradient of the rotating magnetic field in the axial direction (z direction) are assumed to be zero.

The applied external rotating magnetic field in the Cartesian coordinate system is

$$\vec{B} = B_0\left[(\cos\omega t\cdot\vec{e}_x + \sin\omega t\cdot\vec{e}_y\right], \tag{1}$$

where $\vec{e}_x, \vec{e}_y$ are unit vectors in the x and y directions, respectively.

The rotating magnetic distribution, as express by equation (1), does not depend on (x, y); when the skin effect is considered, as in the present study, the rotating magnetic field is reduced into the melt, the magnetic field depends on (x, y), and its distribution is given by the solution of the following advection-diffusion equation:

$$\frac{\partial\vec{B}}{\partial t} = \nabla\times(\vec{U}\times\vec{B}) + \frac{1}{\mu\sigma}\nabla^2\vec{B},$$

where $\vec{U}$ is the fluid velocity and μ is the melt permeability. The first term in the right represents the magnetic flux density varies with fluid flow, and this term is ignored as in [15]. Thus, the above advection-diffusion equation is simplified as

$$\frac{\partial\vec{B}}{\partial t} = \frac{1}{\mu\sigma}\nabla^2\vec{B}. \tag{2}$$

In addition, the magnetic field satisfies

$$\nabla\cdot\vec{B} = 0. \tag{3}$$

To calculate the distribution of magnetic field in melt, the cylindrical coordinate system is adopted. The following complex variables are introduced, where the real part corresponds to the physical quantities. As $r\to\infty$, the imposed magnetic field is written as

$$\vec{B}_{r\to\infty} = B_0 e^{i(\omega t-\theta)}(\vec{e}_r - i\vec{e}_\theta), \tag{4}$$

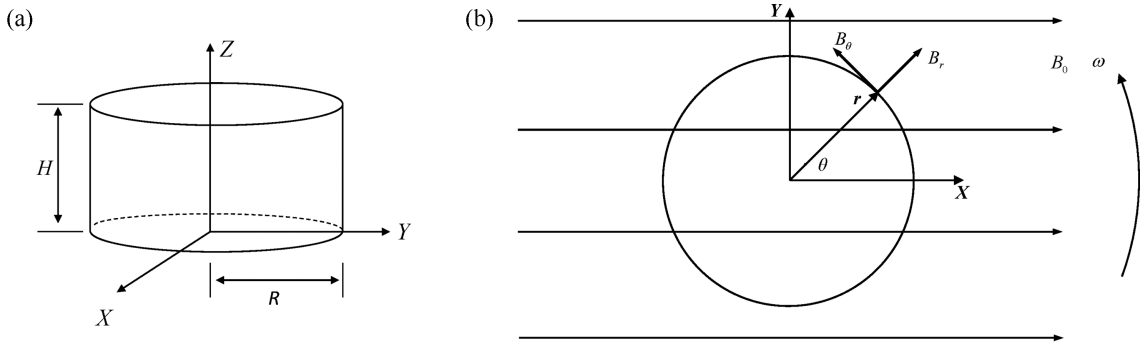

Fig. 1. (a) Liquid bridge model, and (b) external rotating magnetic field.

where, t denotes time, θ is angular coordinate, i, with $i^2 = -1$, is imaginary unit, $\vec{e_r}$ and $\vec{e_\theta}$ are unit vectors in radial and azimuthal directions, respectively.

Equation (3) can be written in cylindrical coordinate system as,

$$\frac{\partial}{\partial r}(rB_r) + \frac{\partial B_\theta}{\partial \theta} = 0 , \tag{5}$$

Combining (2) and (5) in cylindrical coordinate system, we obtain

$$\frac{\partial}{\partial t}(rB_r) = \frac{1}{\sigma\mu}\left[\frac{1}{r}\frac{\partial}{\partial r}(rB_r) + \frac{\partial^2}{\partial r^2}(rB_r) + \frac{1}{r^2}\frac{\partial^2}{\partial \theta^2}(rB_r)\right]. \tag{6}$$

From the equation (4), an approximate boundary condition at $r = R$ is determined as

$$B_r\big|_{r=R} = B_0 \mathrm{e}^{i(\omega t-\theta)} . \tag{7}$$

Based on the equation (6), B_r is assumed in the form as

$$B_r = \frac{\mathrm{f}}{r} e^{i(\omega t-\theta)} , \tag{8}$$

where f is a function of r. From equations (5) and (8), we derive

$$B_\theta = -i\frac{d\,\mathrm{f}}{dr} e^{i(\omega t-\theta)} . \tag{9}$$

Substituting equation (8) into equation (6), the equation for f becomes

$$r^2\frac{d^2\,\mathrm{f}}{dr^2} + r\frac{d\,\mathrm{f}}{dr} - \left[i\sigma\mu\omega r^2 + 1\right]\mathrm{f} = 0 . \tag{10}$$

Defined $\beta = \sqrt{\sigma\mu\omega}e^{3\pi i/4}$, the equation (10) is written as

$$r^2\frac{d^2\,\mathrm{f}}{dr^2} + r\frac{d\,\mathrm{f}}{dr} + \left[(\beta r)^2 - 1\right]\mathrm{f} = 0 . \tag{11}$$

With definition of a new independent variable $\hat{r} = \beta r$, the equation (11) becomes

$$\hat{r}^2\frac{d^2\,\mathrm{f}}{d\hat{r}^2} + \hat{r}\frac{d\,\mathrm{f}}{d\hat{r}} + \left[\hat{r}^2 - 1\right]\mathrm{f} = 0 , \tag{12}$$

it is a standard Bessel equation, and the boundary condition for f is derived from (7) and (8) as $\mathrm{f}\big|_{r=R} = B_0 R$.

The equation (12) is solved with Bessel functions as

$$\mathrm{f} = \frac{RB_0 J_1\left(\frac{\sqrt{K}}{R} r\sqrt{-i}\right)}{J_1(\sqrt{K}\sqrt{-i})} .$$

Then, the solution of the magnetic field distribution in the form of Bessel functions is obtained as

$$B_r = \frac{RB_0 J_1\left(\frac{\sqrt{K}}{R} r\sqrt{-i}\right)}{rJ_1(\sqrt{K}\sqrt{-i})} \cdot e^{i(\omega t-\theta)} , \tag{13}$$

$$B_\theta = -ie^{i(\omega t-\theta)} \cdot \frac{d}{dr}\left(\frac{RB_0 J_1\left(\frac{\sqrt{K}}{R} r\sqrt{-i}\right)}{J_1(\sqrt{K}\sqrt{-i})}\right) . \tag{14}$$

The physical values of B_r and B_θ are the real parts of the equations (13) and (14), i.e.

$$B_r = \mathrm{Re}\left(\frac{RB_0}{r}\frac{ber_1\left(\frac{\sqrt{K}}{R} r\right) + ibei_1\left(\frac{\sqrt{K}}{R} r\right)}{ber_1(\sqrt{K}) + ibei_1(\sqrt{K})} \cdot e^{i(\omega t-\theta)}\right), \tag{15}$$

$$B_\theta = \mathrm{Re}\left(-ie^{i(\omega t-\theta)} \cdot \frac{d}{dr}\left(RB_0 \frac{ber_1\left(\frac{\sqrt{K}}{R} r\right) + ibei_1\left(\frac{\sqrt{K}}{R} r\right)}{ber_1(\sqrt{K}) + ibei_1(\sqrt{K})}\right)\right). \tag{16}$$

Here, the Kelvin functions $ber_1(x)$ and $bei_1(x)$ are the real and imaginary parts, respectively, of $J_1(x\sqrt{-i})$, where x is real and $J_1(x\sqrt{-i})$ is the first order Bessel function of the first kind.

In order to model the interaction of the rotating magnetic field and melt convection, the above distribution of magnetic field is introduced into Φ_1-Φ_2 model. To facilitate calculating the Lorenz force and programming the rotating magnetic field Φ_1-Φ_2 model, the Cartesian coordinate is adopted, and the power series expansion of the analytic solution (i.e. Eqs. (15-16)) is truncated with reserving different terms. In this study, we reserve only the first four terms in the power series expansions of the Kelvin functions as

$$ber_1(x) = \mathrm{Re}[J_1(x\sqrt{-i})] = -\frac{1}{\sqrt{2}}\left[\frac{x}{2} + \frac{(x/2)^3}{1!2!} - \frac{(x/2)^5}{2!3!} - \frac{(x/2)^7}{3!4!}\right],$$

$$bei_1(x) = \mathrm{Im}[J_1(x\sqrt{-i})] = -\frac{1}{\sqrt{2}}\left[-\frac{x}{2} + \frac{(x/2)^3}{1!2!} + \frac{(x/2)^5}{2!3!} - \frac{(x/2)^7}{3!4!}\right].$$

As our analysis in [16], above truncation of first four terms is applicable for $K \le 8$. In the Cartesian coordinate system, the magnetic field with the skin effect is derived as

$$\vec{B}_{rot}(x,y,t)=\frac{B_0}{2+\frac{K^2}{96}+\frac{2K^6}{9216^2}}\begin{bmatrix}(\sin\omega t\cdot B_{x\sin}+\cos\omega t\cdot B_{x\cos})\vec{e}_x\\+(\sin\omega t\cdot B_{y\sin}+\cos\omega t\cdot B_{y\cos})\vec{e}_y\end{bmatrix}, \quad (17)$$

where $B_{x\sin}$, $B_{x\cos}$, $B_{y\sin}$ and $B_{y\cos}$ are derived in Appendix A.

2.1. Rotating magnetic field Φ_1-Φ_2 model without the skin effect

The Lorentz force is obtained by $\vec{f}=\vec{j}\times\vec{B}$, where the current density $\vec{j}$ is determined by $\vec{j}=\sigma(\vec{E}+\vec{U}\times\vec{B})$. In rotating magnetic field, the electric field $\vec{E}$ is derived from $\nabla\times\vec{E}=-\partial\vec{B}/\partial t$ and $\vec{B}=\nabla\times\vec{A}$ as

$$\vec{E}=-\nabla\phi+(B_0\omega x\cdot\cos\omega t+B_0\omega y\cdot\sin\omega t)\vec{e}_z. \quad (18)$$

The electric field $\vec{E}$, the vector potential $\vec{A}$, the current density $\vec{j}$ and the scalar electrical potential ϕ depend on the angular frequency ω. In particular, ϕ is split into two parts as in [3, 5]:

$$\phi(x,y,z,t)=\phi_1(x,y,z)\sin(\omega t)+\phi_2(x,y,z)\cos(\omega t).$$

The Lorentz force includes both time-independent and time-dependent terms, the time-dependent term rotates at an angular frequency of 2ω. Since the melt flow cannot respond quickly at the angular frequency 2ω, the Lorentz force is taken as a time average of one rotation period, and therefore only the time-independent term of the Lorentz force is preserved as in [3, 6, 8]. The components of the Lorentz force are

$$f_x=-\frac{1}{2}\sigma\omega B_0^2y+\frac{1}{2}\sigma B_0\frac{\partial\phi_1}{\partial z}-\frac{1}{2}\sigma B_0^2u, \quad (19)$$

$$f_y=\frac{1}{2}\sigma\omega B_0^2x-\frac{1}{2}\sigma B_0\frac{\partial\phi_2}{\partial z}-\frac{1}{2}\sigma B_0^2v, \quad (20)$$

$$f_z=\frac{1}{2}\sigma B_0\left(\frac{\partial\phi_2}{\partial y}-\frac{\partial\phi_1}{\partial x}\right)-\sigma B_0^2w. \quad (21)$$

Wherein, u, v and w are components of the velocity in x, y, z directions, respectively.

Taking $\nabla\cdot\vec{j}=0$, the governing equation of scalar electric potential is derived as

$$\nabla^2\phi_1=B_0\left(\frac{\partial u}{\partial z}-\frac{\partial w}{\partial x}\right), \quad (22)$$

$$\nabla^2\phi_2=B_0\left(\frac{\partial w}{\partial y}-\frac{\partial v}{\partial z}\right). \quad (23)$$

Electrically insulating boundaries are assumed to surround the liquid bridge, and the boundary condition is derived from $\vec{j}\cdot\vec{n}=0$ with the unit normal vector directing outside of the boundaries $\vec{n}$.

The melt is taken as incompressible Newtonian fluid with constant viscosity η and density ρ. Moreover, this study concentrates on the influence of rotating magnetic field, and the buoyancy and thermocapillary convections are ignored. Employing R and κ/R as the scale of length and velocity, the dimensionless governing equations are derived as:

$$\nabla\cdot\vec{U}^*=0, \quad (24)$$

$$\frac{1}{\mathrm{Pr}}\left(\frac{\partial\vec{U}^*}{\partial t^*}+(\vec{U}^*\cdot\nabla)\vec{U}^*\right)=-\nabla P^*+\nabla^2\vec{U}^*+\vec{f}^*_{Lorz}. \quad (25)$$

$$\frac{\partial T^*}{\partial t^*}+(\vec{U}^*\cdot\nabla)T^*-\nabla^2T^*=0 \quad (26)$$

where $\vec{U}^*=(R/\kappa)\vec{U}$, $t^*=(\kappa/R^2)t$, $p^*=(R^2/\kappa\eta)p$, $\phi^*=(1/B_0\kappa)\phi$. κ and σ are thermal diffusion coefficient and the electrical conductivity, respectively.

The Prandtl, rotation Reynolds and Taylor numbers are defined as

$$\mathrm{Pr}=\frac{\upsilon}{\kappa},\ \mathrm{Re}_\omega=\frac{\omega R^2}{\upsilon}\ \text{and}\ \mathrm{Ta}=\frac{\sigma {B_0}^2\omega R^4}{2\upsilon\eta},$$

where υ is the kinematic viscosity with $\upsilon=\eta/\rho$.

Three components of the dimensionless Lorentz force in the rotating magnetic field $\Phi_1-\Phi_2$ model without the skin effect are

$$f_x^*=\mathrm{Ta}\,\mathrm{Pr}\left[-y^*+\frac{1}{\mathrm{Re}_\omega\,\mathrm{Pr}}\left(\frac{\partial\phi_1^*}{\partial z^*}-u^*\right)\right], \quad (27)$$

$$f_y^*=\mathrm{Ta}\,\mathrm{Pr}\left[x^*-\frac{1}{\mathrm{Re}_\omega\,\mathrm{Pr}}\left(\frac{\partial\phi_2^*}{\partial z^*}+v^*\right)\right], \quad (28)$$

$$f_z^*=\frac{\mathrm{Ta}}{\mathrm{Re}_\omega}\left[\frac{\partial\phi_2^*}{\partial y^*}-\frac{\partial\phi_1^*}{\partial x^*}-2w^*\right], \quad (29)$$

where (u^*,v^*,w^*) and (f_x^*,f_y^*,f_z^*) are the dimensionless velocity and Lorentz force in the Cartesian coordinate system, respectively.

The dimensionless governing equations of scalar electric potential become

$$\nabla^2\phi_1^*=\frac{\partial u^*}{\partial z^*}-\frac{\partial w^*}{\partial x^*}, \quad (30)$$

$$\nabla^2\phi_2^*=\frac{\partial w^*}{\partial y^*}-\frac{\partial v^*}{\partial z^*}. \quad (31)$$

The boundary conditions for the electric potential are determined by $\vec{j}\cdot\vec{n}=0$, as

$$\frac{\partial\phi_1^*}{\partial n^*}=\left[-w^*\vec{e}_x+(\mathrm{Re}_\omega\,\mathrm{Pr}\cdot y^*+u^*)\vec{e}_z\right]\cdot\vec{n}, \quad (32)$$

$$\frac{\partial\phi_2^*}{\partial n^*}=\left[w^*\vec{e}_y+(\mathrm{Re}_\omega\,\mathrm{Pr}\cdot x^*-v^*)\vec{e}_z\right]\cdot\vec{n}\cdot \quad (33)$$

2.2. Rotating magnetic field Φ_1-Φ_2 model with the skin effect

To investigate the influence of the skin effect in rotating magnetic field, the rotating magnetic field as in equation (17) is applied to the cylindrical liquid bridge. The dimensionless components of the Lorentz force are derived as:

$$\begin{aligned}f_x^*=&\frac{\mathrm{Ta}}{C\cdot\mathrm{Re}_\omega}\left(\frac{\partial\phi_1^*}{\partial z^*}\hat{B}_{y\sin}+\frac{\partial\phi_2^*}{\partial z^*}\hat{B}_{y\cos}\right)\\&+\frac{\mathrm{Ta}}{C^2\cdot\mathrm{Re}_\omega}[v^*(\hat{B}_{x\sin}\cdot\hat{B}_{y\sin}+\hat{B}_{x\cos}\cdot\hat{B}_{y\cos}),\\&\qquad -u^*(\hat{B}_{y\sin}{}^2+\hat{B}_{y\cos}{}^2)]\\&-\frac{\mathrm{Ta}\cdot\mathrm{Pr}}{C^2}(\hat{B}_{y\sin}\cdot\hat{A}_{zt\sin}+\hat{B}_{y\cos}\cdot\hat{A}_{zt\cos})\end{aligned} \quad (34)$$

$$\begin{aligned}f_y^*=&-\frac{\mathrm{Ta}}{C\cdot\mathrm{Re}_\omega}\left(\frac{\partial\phi_1^*}{\partial z^*}\hat{B}_{x\sin}+\frac{\partial\phi_2^*}{\partial z^*}\hat{B}_{x\cos}\right)\\&+\frac{\mathrm{Ta}}{C^2\cdot\mathrm{Re}_\omega}[u^*(\hat{B}_{x\sin}\cdot\hat{B}_{y\sin}+\hat{B}_{x\cos}\cdot\hat{B}_{y\cos}),\\&\qquad -v^*(\hat{B}_{x\sin}{}^2+\hat{B}_{x\cos}{}^2)]\\&+\frac{\mathrm{Ta}\cdot\mathrm{Pr}}{C^2}(\hat{B}_{x\sin}\cdot\hat{A}_{zt\sin}+\hat{B}_{x\cos}\cdot\hat{A}_{zt\cos})\end{aligned} \quad (35)$$

$$\begin{aligned}f_z^*=&\frac{\mathrm{Ta}}{C\cdot\mathrm{Re}_\omega}\left(\frac{\partial\phi_1^*}{\partial y^*}\hat{B}_{x\sin}+\frac{\partial\phi_2^*}{\partial y^*}\hat{B}_{x\cos}-\frac{\partial\phi_1^*}{\partial x^*}\hat{B}_{y\sin}-\frac{\partial\phi_2^*}{\partial x^*}\hat{B}_{y\cos}\right)\\&-\frac{\mathrm{Ta}}{C^2\cdot\mathrm{Re}_\omega}w^*(\hat{B}_{y\sin}{}^2+\hat{B}_{y\cos}{}^2+\hat{B}_{x\sin}{}^2+\hat{B}_{x\cos}{}^2)\end{aligned} \quad . (36)$$

Taking $\nabla\cdot\vec{j}=0$, the dimensionless governing equation of scalar electric potential is derived as:

$$\nabla^2\phi_1^*=\frac{1}{C}\left[\hat{B}_{y\sin}\left(\frac{\partial u^*}{\partial z^*}-\frac{\partial w^*}{\partial x^*}\right)+\hat{B}_{x\sin}\left(\frac{\partial w^*}{\partial y^*}-\frac{\partial v^*}{\partial z^*}\right)+w^*\hat{\phi}_{1\sin}\right], \quad (37)$$

$$\nabla^2\phi_2^*=\frac{1}{C}\left[\hat{B}_{y\cos}\left(\frac{\partial u^*}{\partial z^*}-\frac{\partial w^*}{\partial x^*}\right)+\hat{B}_{x\cos}\left(\frac{\partial w^*}{\partial y^*}-\frac{\partial v^*}{\partial z^*}\right)+w^*\hat{\phi}_{2\cos}\right]. \quad (38)$$

The boundary conditions for the electric potential are:

$$\frac{\partial\phi_1^*}{\partial n^*}=\begin{bmatrix}-\frac{1}{C}w^*\cdot\hat{B}_{y\sin}\vec{e}_x+\frac{1}{C}w^*\cdot\hat{B}_{x\sin}\vec{e}_y\\+\frac{1}{C}(u^*\cdot\hat{B}_{y\sin}-v^*\cdot\hat{B}_{x\sin}+\mathrm{Pr}\cdot\mathrm{Re}_\omega\cdot\hat{A}_{zt\sin})\vec{e}_z\end{bmatrix}\cdot\vec{n}, \quad (39)$$

$$\frac{\partial\phi_2^*}{\partial n^*}=\begin{bmatrix}-\frac{1}{C}w^*\cdot\hat{B}_{y\cos}\vec{e}_x+\frac{1}{C}w^*\cdot\hat{B}_{x\cos}\vec{e}_y\\+\frac{1}{C}(u^*\cdot\hat{B}_{y\cos}-v^*\cdot\hat{B}_{x\cos}+\mathrm{Pr}\cdot\mathrm{Re}_\omega\cdot\hat{A}_{zt\cos})\vec{e}_z\end{bmatrix}\cdot\vec{n}. \quad (40)$$

In equations (34)-(40), $C=2+\frac{K^2}{96}+\frac{2K^6}{9216^2}$, and $\hat{B}_{x\sin}$, $\hat{B}_{x\cos}$, $\hat{B}_{y\sin}$, $\hat{B}_{y\cos}$, $\hat{A}_{zt\sin}$, $\hat{A}_{zt\cos}$, $\hat{\phi}_{1\sin}$ and $\hat{\phi}_{2\cos}$ are exhibited in Appendix B.

The velocity and temperature boundary conditions for two models are

Upper boundary: $\vec{U}^*=0$, $T^*=1$;

Lower boundary: $\vec{U}^*=0$, $T^*=0$;

The circumference boundary: the surface is impervious to flows of mass, momentum and energy.

Initial conditions are: $\vec{U}^*=0$, $T^*=0.5$, $\phi_1^*=0$ and $\phi_2^*=0$.

3. Results and Discussion

The dimensionless governing equations (24)-(26) were discretized by the finite volume method. The two-order upwind scheme was applied to the convection term, and the flow field was resolved by the SIMPLE algorithm. The grid convergence was checked as indicated in Table 1, and a non-uniform grid (60 × 68 × 60) was adopted. The dimensionless parameters in the present simulations were Pr = 0.01, H/R = 1, $\mathrm{Re}_\omega=2.2\times10^4$, $\mathrm{Ta}=1.0\times10^4$ and K = 0-8.

In the cylindrical liquid bridge, convection was driven by the rotating magnetic field and the consequent stirring action of the Lorentz force in the azimuthal direction (which is the same direction of the applied rotating magnetic field), and an axisymmetric rotating flow along the liquid bridge axis was observed, as shown in Fig. 2. The convection in the *r*-*z* plane, as exhibited in Figs. 3(a-c), was a two-vortex-pairs structure induced by centrifugal force and pressure gradient. Under the rotating magnetic field, the skin effect leads to a non-uniform magnetic distribution in the melt, and the magnetic field achieves its maximum strength near the melt surface. Thus, in the

Table 1. Dimensionless maximal velocity of flow driven by an rotatng magnetic field without skin effect (Pr = 0.01, $\mathrm{Re}_\omega=2.2\times10^4$, $\mathrm{Ta}=1.0\times10^4$) for difference meshes.

Grid ($n_z\times n_\varphi\times n_r$)	Maximal Velocity	Maximal Azimuthal Velocity
40 × 48 × 40	1.5704	1.567
50 × 60 × 50	1.5869	1.5847
60 × 68 × 60	1.5913	1.5896

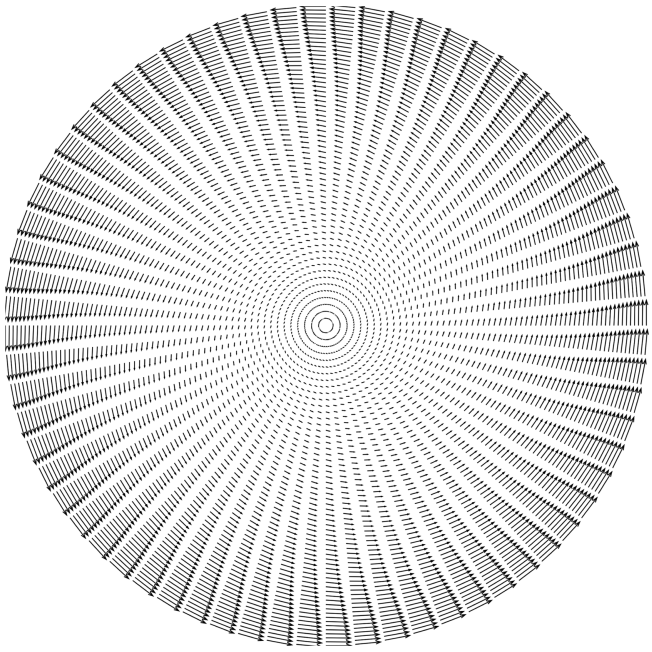

Fig. 2. Velocity vector in $z = 0.5$ generated by rotating magnetic field.

finite length model of the rotating magnetic field, the comparison between the result from the model without the skin effect (i.e. equations (27-29)) and that from the model with the skin effect (i.e. equations (34-36)) indicated an obvious deviation in the azimuthal velocity with increasing dimensionless shielding parameter K, as exhibited in Figs. 3(a-c). Also, an obvious deviation in temperature with increasing dimensionless shielding parameter K was observed, as indicated in Fig. 4.

In the flow driven by the rotating magnetic field, the main flow was in the azimuthal direction, and the secondary flow was relatively weak, which facts are exhibited in Figs. 5-6. Because of the skin effect, the magnetic field cannot penetrate into the melt volume without change, and the magnetic lines bend to the cylinder surface more obviously with increasing K; therefore, in ignoring the skin effect for a large K, an obvious deviation was observed. To quantitatively estimate the error by ignoring the skin effect, the relative error ξ was defined as $\xi = \left|(u_2 - u_1)/u_1\right| \times 100\%$, where u_2 is the velocity considering the skin effect, and u_1 is the velocity without the skin effect. The maximal relative deviation was located near the symmetry axial even though the absolute velocity deviation appeared at the free surface, as shown in Figs. 5(a-c). For $K = 2$, the maximal relative velocity error was 6.1 %, and the maximal relative errors of the radial and azimuthal velocities were 15.9 and 7.7 %, respectively. For $K = 8$, the maximal relative velocity

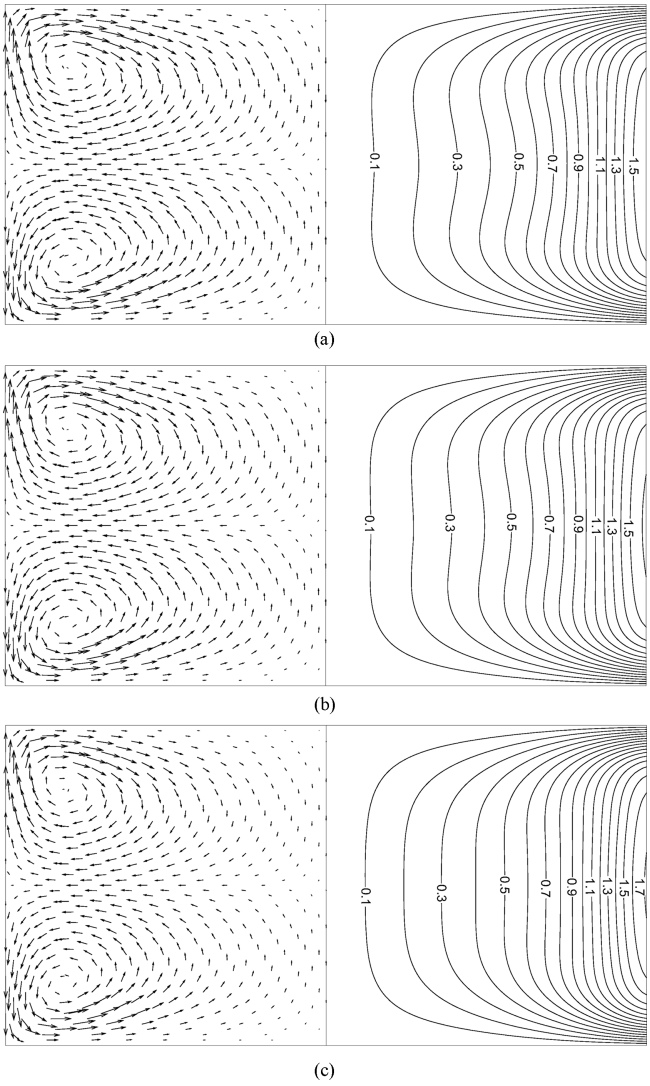

Fig. 3. Velocity vector (left) and azimuthal velocity contours (right) at $x = 0$ for rotating magnetic field $\Phi_1 - \Phi_2$ model: (a) without skin effect, (b) $K = 2$, (c) $K = 8$.

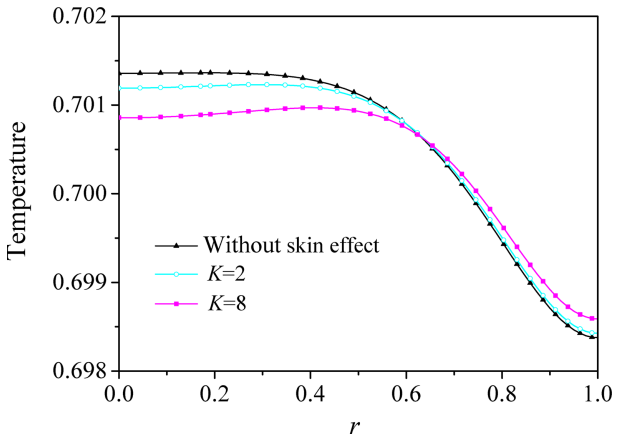

Fig. 4. (Color online) Temperature distribution at $z = 0.7$ for different K.

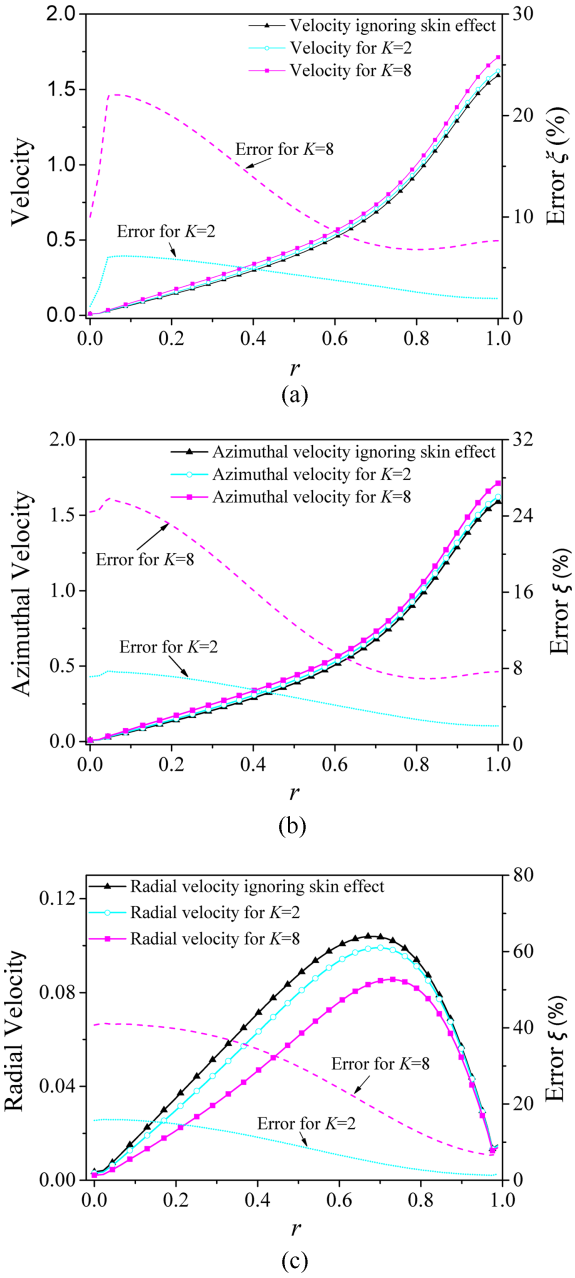

Fig. 5. (Color online) Velocity generated by rotating magnetic field for different K and corresponding error ξ at z = 0.5: (a) velocity magnitude, (b) azimuthal velocity component, and (c) radial velocity component.

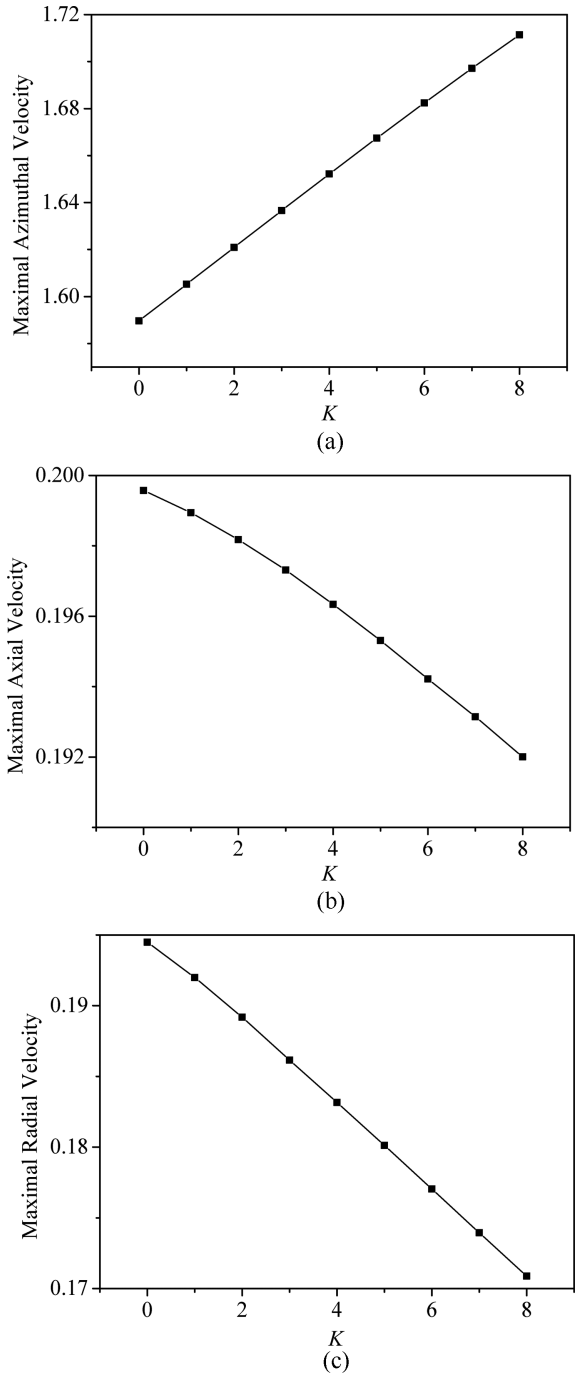

Fig. 6. Maximal velocity for different shielding parameters K: (a) maximal azimuthal velocity component, (b) maximal axial velocity component, (c) maximal radial velocity component.

error was 22.1 %, and the maximal relative errors of the radial and azimuthal velocities are 41.2 and 25.9 %, respectively.

Figs. 6(a-c) illustrate the maximal velocity of melt convection driven by the rotating magnetic field for different K ($K = 0$ for the case ignoring the skin effect). With the rise of K, the maximal azimuthal velocity increased, while the maximal axial and radial velocities decreased. The maximal azimuthal, axial and radial velocities for $K = 8$ were 1.077, 0.962 and 0.879 times those for $K = 0$, respectively. Therefore, the skin effect of the rotating magnetic field cannot be ignored.

4. Conclusion

In terms of Bessel functions, an analytical solution for the distribution of the rotating magnetic field was derived, and the first four terms in the power series expansions of the Kelvin functions were adopted. Then the rotating magnetic field Φ_1-Φ_2 model with the skin effect was proposed. The flow driven by the rotating magnetic field was simulated numerically, and the influence of the skin effect was investigated. The results indicate that an obvious deviation in velocity appears when the skin effect is ignored. The rotating magnetic field model ignoring the skin effect leads to a smaller azimuthal velocity and larger radial and axial velocity components.

Acknowledgments

This work is supported by the National Natural Science Foundation of China (No. 11572062), the Fundamental Research Funds for the Central Universities (CDJXS11240013), and Program for Changjiang Scholars and Innovative Research Team in University (No. IRT13043). Zeng would like to thank the support of Key Laboratory of Functional Crystals and Laser Technology, TIPC, CAS.

Appendix A

From the equation (15) and (16), the distribution of rotating magnetic field with the skin effect in melt are

$$B_r = \mathrm{Re}\left(\frac{RB_0}{r}\frac{ber_1(\frac{\sqrt{K}}{R}r)+ibei_1(\frac{\sqrt{K}}{R}r)}{ber_1(\sqrt{K})+ibei_1(\sqrt{K})}\cdot e^{i(\omega t-\theta)}\right)$$

$$B_\theta = \mathrm{Re}\left(-ie^{i(\omega t-\theta)}\cdot\frac{d}{dr}\left(RB_0\frac{ber_1(\frac{\sqrt{K}}{R}r)+ibei_1(\frac{\sqrt{K}}{R}r)}{ber_1(\sqrt{K})+ibei_1(\sqrt{K})}\right)\right)$$

In this study, the first four terms in the power series expansions of the Kelvin functions are reserved,

$$ber_1(\frac{\sqrt{K}}{R}r) = -\frac{1}{\sqrt{2}}\left[\frac{\sqrt{K}}{2R}r+\frac{(\frac{\sqrt{K}}{2R}r)^3}{1!2!}-\frac{(\frac{\sqrt{K}}{2R}r)^5}{2!3!}-\frac{(\frac{\sqrt{K}}{2R}r)^7}{3!4!}\right]$$

$$bei_1(\frac{\sqrt{K}}{R}r) = -\frac{1}{\sqrt{2}}\left[-\frac{\sqrt{K}}{2R}r+\frac{(\frac{\sqrt{K}}{2R}r)^3}{1!2!}+\frac{(\frac{\sqrt{K}}{2R}r)^5}{2!3!}-\frac{(\frac{\sqrt{K}}{2R}r)^7}{3!4!}\right]$$

$$ber_1(\sqrt{K}) = -\frac{1}{\sqrt{2}}\left[\frac{\sqrt{K}}{2}+\frac{(\frac{\sqrt{K}}{2})^3}{1!2!}-\frac{(\frac{\sqrt{K}}{2})^5}{2!3!}-\frac{(\frac{\sqrt{K}}{2})^7}{3!4!}\right]$$

$$bei_1(\sqrt{K}) = -\frac{1}{\sqrt{2}}\left[-\frac{\sqrt{K}}{2}+\frac{(\frac{\sqrt{K}}{2})^3}{1!2!}+\frac{(\frac{\sqrt{K}}{2})^5}{2!3!}-\frac{(\frac{\sqrt{K}}{2})^7}{3!4!}\right]$$

Hence,

$$B_r = \frac{B_0}{2+\frac{K^2}{96}+\frac{2K^6}{9216^2}}\left\{\begin{array}{l}\sin(\omega t-\theta)\left[\begin{array}{l}\frac{K}{4}-\frac{K^3}{4608}+\frac{1}{R^2}(\frac{K^3}{768}-\frac{K}{4})r^2\\+\frac{1}{R^4}(\frac{K^5}{884736}-\frac{K^3}{768})r^4\\+\frac{1}{R^6}(\frac{K^3}{4608}-\frac{K^5}{884736})r^6\end{array}\right]\\+\cos(\omega t-\theta)\left[\begin{array}{l}2-\frac{K^2}{96}+\frac{1}{R^2}(\frac{K^2}{32}-\frac{K^4}{36864})r^2\\+\frac{1}{R^4}(\frac{2K^4}{192^2}-\frac{K^2}{96})r^4\\+\frac{1}{R^6}(\frac{2K^6}{9216^2}-\frac{K^4}{36864})r^6\end{array}\right]\end{array}\right\}$$

$$B_\theta = -\frac{B_0}{2+\frac{K^2}{96}+\frac{2K^6}{9216^2}}\left\{\begin{array}{l}\cos(\omega t-\theta)\left[\begin{array}{l}\frac{K}{4}-\frac{K^3}{4608}+\frac{3}{R^2}(\frac{K^3}{768}-\frac{K}{4})r^2\\+\frac{5}{R^4}(\frac{K^5}{884736}-\frac{K^3}{768})r^4\\+\frac{7}{R^6}(\frac{K^3}{4608}-\frac{K^5}{884736})r^6\end{array}\right]\\-\sin(\omega t-\theta)\left[\begin{array}{l}2-\frac{K^2}{96}+\frac{3}{R^2}(\frac{K^2}{32}-\frac{K^4}{36864})r^2\\+\frac{5}{R^4}(\frac{2K^4}{192^2}-\frac{K^2}{96})r^4\\+\frac{7}{R^6}(\frac{2K^6}{9216^2}-\frac{K^4}{36864})r^6\end{array}\right]\end{array}\right\}$$

The magnetic field with the skin effect in the melt in the Cartesian coordinate system is transformed from $B_x = B_r\cos\theta - B_\theta\sin\theta$, $B_y = B_r\sin\theta + B_\theta\cos\theta$, $x = r\cos\theta$ and $y = r\sin\theta$, hence

$$B_x = \frac{B_0}{2+\frac{K^2}{96}+\frac{2K^6}{9216^2}}\left\{\begin{array}{l}\sin\omega t\left[\begin{array}{l}\frac{K}{4}-\frac{K^3}{4608}+\frac{1}{R^2}(\frac{K^3}{768}-\frac{K}{4})(x^2+3y^2)\\+\frac{1}{R^4}(\frac{K^5}{884736}-\frac{K^3}{768})(x^2+y^2)(x^2+5y^2)\\+\frac{1}{R^6}(\frac{K^3}{4608}-\frac{K^5}{884736})(x^2+y^2)^2(x^2+7y^2)\\-\frac{1}{R^2}(\frac{K^2}{16}-\frac{K^4}{18432})xy\\-\frac{1}{R^4}(\frac{8K^4}{192^2}-\frac{K^2}{24})(x^2+y^2)xy\\-\frac{1}{R^6}(\frac{12K^6}{9216^2}-\frac{K^4}{6144})(x^2+y^2)^2xy\end{array}\right]\\+\cos\omega t\left[\begin{array}{l}2-\frac{K^2}{96}+\frac{1}{R^2}(\frac{K^2}{32}-\frac{K^4}{36864})(x^2+3y^2)\\+\frac{1}{R^4}(\frac{2K^4}{192^2}-\frac{K^2}{96})(x^2+y^2)(x^2+5y^2)\\+\frac{1}{R^6}(\frac{2K^6}{9216^2}-\frac{K^4}{36864})(x^2+y^2)^2(x^2+7y^2)\\+\frac{1}{R^2}(\frac{K^3}{384}-\frac{K}{2})xy\\+\frac{1}{R^4}(\frac{K^5}{221184}-\frac{K^3}{192})(x^2+y^2)xy\\+\frac{1}{R^6}(\frac{K^3}{768}-\frac{K^5}{147456})(x^2+y^2)^2xy\end{array}\right]\end{array}\right\}$$

$$B_y = \frac{B_0}{2+\frac{K^2}{96}+\frac{2K^6}{9216^2}} \left\{ \begin{array}{l} \sin\omega t \left[\begin{array}{l} 2-\frac{K^2}{96}+\frac{1}{R^2}(\frac{K^2}{32}-\frac{K^4}{36864})(3x^2+y^2) \\ +\frac{1}{R^4}(\frac{2K^4}{192^2}-\frac{K^2}{96})(x^2+y^2)(5x^2+y^2) \\ +\frac{1}{R^6}(\frac{2K^6}{9216^2}-\frac{K^4}{36864})(x^2+y^2)^2(7x^2+y^2) \\ -\frac{1}{R^2}(\frac{K^3}{384}-\frac{K}{2})xy \\ -\frac{1}{R^4}(\frac{K^5}{221184}-\frac{K^3}{192})(x^2+y^2)xy \\ -\frac{1}{R^6}(\frac{K^3}{768}-\frac{K^5}{147456})(x^2+y^2)^2xy \end{array} \right] \\ +\cos\omega t \left[\begin{array}{l} -(\frac{K}{4}-\frac{K^3}{4608})-\frac{1}{R^2}(\frac{K^3}{768}-\frac{K}{4})(3x^2+y^2) \\ -\frac{1}{R^4}(\frac{K^5}{884736}-\frac{K^3}{768})(x^2+y^2)(5x^2+y^2) \\ -\frac{1}{R^6}(\frac{K^3}{4608}-\frac{K^5}{884736})(x^2+y^2)^2(7x^2+y^2) \\ -\frac{1}{R^2}(\frac{K^2}{16}-\frac{K^4}{18432})xy \\ -\frac{1}{R^4}(\frac{8K^4}{192^2}-\frac{K^2}{24})(x^2+y^2)xy \\ -\frac{1}{R^6}(\frac{12K^6}{9216^2}-\frac{K^4}{6144})(x^2+y^2)^2xy \end{array} \right] \end{array} \right\}$$

The magnetic field with the skin effect in the melt is denoted as

$$\vec{B}_{rot}(x,y,t) = \frac{B_0}{2+\frac{K^2}{96}+\frac{2K^6}{9216^2}} \left[\begin{array}{l} (\sin\omega t \cdot B_{x\sin} + \cos\omega t \cdot B_{x\cos})\vec{e}_x \\ +(\sin\omega t \cdot B_{y\sin} + \cos\omega t \cdot B_{y\cos})\vec{e}_y \end{array} \right]$$

where $B_{x\sin}$, $B_{x\cos}$, $B_{y\sin}$ and $B_{y\cos}$ are described as

$$\begin{aligned} B_{x\sin} = & \frac{K}{4}-\frac{K^3}{4608}+\frac{1}{R^2}(\frac{K^3}{768}-\frac{K}{4})(x^2+3y^2) \\ & +\frac{1}{R^4}(\frac{K^5}{884736}-\frac{K^3}{768})(x^2+y^2)(x^2+5y^2) \\ & +\frac{1}{R^6}(\frac{K^3}{4608}-\frac{K^5}{884736})(x^2+y^2)^2(x^2+7y^2) \\ & -\frac{1}{R^2}(\frac{K^2}{16}-\frac{K^4}{18432})xy-\frac{1}{R^4}(\frac{8K^4}{192^2}-\frac{K^2}{24})(x^2+y^2)xy \\ & -\frac{1}{R^6}(\frac{12K^6}{9216^2}-\frac{K^4}{6144})(x^2+y^2)^2xy \end{aligned}$$

$$\begin{aligned} B_{x\cos} = & 2-\frac{K^2}{96}+\frac{1}{R^2}(\frac{K^2}{32}-\frac{K^4}{36864})(x^2+3y^2) \\ & +\frac{1}{R^4}(\frac{2K^4}{192^2}-\frac{K^2}{96})(x^2+y^2)(x^2+5y^2) \\ & +\frac{1}{R^6}(\frac{2K^6}{9216^2}-\frac{K^4}{36864})(x^2+y^2)^2(x^2+7y^2) \\ & +\frac{1}{R^2}(\frac{K^3}{384}-\frac{K}{2})xy+\frac{1}{R^4}(\frac{K^5}{221184}-\frac{K^3}{192})(x^2+y^2)xy \\ & +\frac{1}{R^6}(\frac{K^3}{768}-\frac{K^5}{147456})(x^2+y^2)^2xy \end{aligned}$$

$$\begin{aligned} B_{y\sin} = & 2-\frac{K^2}{96}+\frac{1}{R^2}(\frac{K^2}{32}-\frac{K^4}{36864})(3x^2+y^2) \\ & +\frac{1}{R^4}(\frac{2K^4}{192^2}-\frac{K^2}{96})(x^2+y^2)(5x^2+y^2) \\ & +\frac{1}{R^6}(\frac{2K^6}{9216^2}-\frac{K^4}{36864})(x^2+y^2)^2(7x^2+y^2) \\ & -\frac{1}{R^2}(\frac{K^3}{384}-\frac{K}{2})xy-\frac{1}{R^4}(\frac{K^5}{221184}-\frac{K^3}{192})(x^2+y^2)xy \\ & -\frac{1}{R^6}(\frac{K^3}{768}-\frac{K^5}{147456})(x^2+y^2)^2xy \end{aligned}$$

$$\begin{aligned} B_{y\cos} = & -(\frac{K}{4}-\frac{K^3}{4608})-\frac{1}{R^2}(\frac{K^3}{768}-\frac{K}{4})(3x^2+y^2) \\ & -\frac{1}{R^4}(\frac{K^5}{884736}-\frac{K^3}{768})(x^2+y^2)(5x^2+y^2) \\ & -\frac{1}{R^6}(\frac{K^3}{4608}-\frac{K^5}{884736})(x^2+y^2)^2(7x^2+y^2) \\ & -\frac{1}{R^2}(\frac{K^2}{16}-\frac{K^4}{18432})xy-\frac{1}{R^4}(\frac{8K^4}{192^2}-\frac{K^2}{24})(x^2+y^2)xy \\ & -\frac{1}{R^6}(\frac{12K^6}{9216^2}-\frac{K^4}{6144})(x^2+y^2)^2xy \end{aligned}$$

Appendix B

The following functions are functions of dimensionless x^*, y^*, and the symbol of "*" is omitted for the sake of convenience.

In calculating the dimensionless Lorentz force by the rotating magnetic field with the skin effect $\vec{B}_{rot}(x,y,t)$,

$$\begin{aligned} \hat{B}_{x\sin} = & \frac{K}{4}-\frac{K^3}{4608}+(\frac{K^3}{768}-\frac{K}{4})(x^2+3y^2) \\ & +(\frac{K^5}{884736}-\frac{K^3}{768})(x^2+y^2)(x^2+5y^2) \\ & +(\frac{K^3}{4608}-\frac{K^5}{884736})(x^2+y^2)^2(x^2+7y^2) \\ & -(\frac{K^2}{16}-\frac{K^4}{18432})xy-(\frac{8K^4}{192^2}-\frac{K^2}{24})(x^2+y^2)xy \\ & -(\frac{12K^6}{9216^2}-\frac{K^4}{6144})(x^2+y^2)^2xy \end{aligned}$$

$$\begin{aligned} \hat{B}_{x\cos} = & 2-\frac{K^2}{96}+(\frac{K^2}{32}-\frac{K^4}{36864})(x^2+3y^2) \\ & +(\frac{2K^4}{192^2}-\frac{K^2}{96})(x^2+y^2)(x^2+5y^2) \\ & +(\frac{2K^6}{9216^2}-\frac{K^4}{36864})(x^2+y^2)^2(x^2+7y^2) \\ & +(\frac{K^3}{384}-\frac{K}{2})xy+(\frac{K^5}{221184}-\frac{K^3}{192})(x^2+y^2)xy \\ & +(\frac{K^3}{768}-\frac{K^5}{147456})(x^2+y^2)^2xy \end{aligned}$$

$$\hat{B}_{y\sin}=2-\frac{K^2}{96}+(\frac{K^2}{32}-\frac{K^4}{36864})(3x^2+y^2)$$
$$+(\frac{2K^4}{192^2}-\frac{K^2}{96})(x^2+y^2)(5x^2+y^2)$$
$$+(\frac{2K^6}{9216^2}-\frac{K^4}{36864})(x^2+y^2)^2(7x^2+y^2)$$
$$-(\frac{K^3}{384}-\frac{K}{2})xy-(\frac{K^5}{221184}-\frac{K^3}{192})(x^2+y^2)xy$$
$$-(\frac{K^3}{768}-\frac{K^5}{147456})(x^2+y^2)^2xy$$

$$\hat{B}_{y\cos}=-(\frac{K}{4}-\frac{K^3}{4608})-(\frac{K^3}{768}-\frac{K}{4})(3x^2+y^2)$$
$$-(\frac{K^5}{884736}-\frac{K^3}{768})(x^2+y^2)(5x^2+y^2)$$
$$-(\frac{K^3}{4608}-\frac{K^5}{884736})(x^2+y^2)^2(7x^2+y^2)$$
$$-(\frac{K^2}{16}-\frac{K^4}{18432})xy-(\frac{8K^4}{192^2}-\frac{K^2}{24})(x^2+y^2)xy$$
$$-(\frac{12K^6}{9216^2}-\frac{K^4}{6144})(x^2+y^2)^2xy$$

$$\hat{\phi}_{1\sin}=(\frac{K^3}{96}-2K)y-(\frac{K^2}{4}-\frac{K^4}{4608})x$$
$$+(\frac{K^5}{36864}-\frac{K^3}{32})(x^2+y^2)y+(\frac{K^3}{96}-\frac{K^5}{18432})(x^2+y^2)^2y$$
$$-(\frac{K^4}{768}-\frac{K^2}{4})(x^2+y^2)x-(\frac{96K^6}{9216^2}-\frac{K^4}{768})(x^2+y^2)^2x$$

$$\hat{\phi}_{2\cos}=(\frac{K^3}{96}-2K)x+(\frac{K^2}{4}-\frac{K^4}{4608})y$$
$$+(\frac{K^5}{36864}-\frac{K^3}{32})(x^2+y^2)x+(\frac{K^3}{96}-\frac{K^5}{18432})(x^2+y^2)^2x$$
$$+(\frac{K^4}{768}-\frac{K^2}{4})(x^2+y^2)y+(\frac{96K^6}{9216^2}-\frac{K^4}{768})(x^2+y^2)^2y$$

$$\hat{A}_{zt\sin}=(\frac{K}{4}-\frac{K^3}{4608})x+(2-\frac{K^2}{96})y$$
$$+(\frac{K^2}{32}-\frac{K^4}{36864})(x^2+y^2)y+(\frac{2K^4}{192^2}-\frac{K^2}{96})(x^2+y^2)^2y$$
$$+(\frac{2K^6}{9216^2}-\frac{K^4}{36864})(x^2+y^2)^3y$$
$$+(\frac{K^3}{768}-\frac{K}{4})(x^2+y^2)x+(\frac{K^5}{884736}-\frac{K^3}{768})(x^2+y^2)^2x$$
$$+(\frac{K^3}{4608}-\frac{K^5}{884736})(x^2+y^2)^3x$$

$$\hat{A}_{zt\cos}=(2-\frac{K^2}{96})x-(\frac{K}{4}-\frac{K^3}{4608})y$$
$$+(\frac{K^2}{32}-\frac{K^4}{36864})(x^2+y^2)x+(\frac{2K^4}{192^2}-\frac{K^2}{96})(x^2+y^2)^2x$$
$$+(\frac{2K^6}{9216^2}-\frac{K^4}{36864})(x^2+y^2)^3x$$
$$-(\frac{K^3}{768}-\frac{K}{4})(x^2+y^2)y-(\frac{K^5}{884736}-\frac{K^3}{768})(x^2+y^2)^2y$$
$$-(\frac{K^3}{4608}-\frac{K^5}{884736})(x^2+y^2)^3y$$

Nomenclature

R	: Radius of the liquid bridge
H	: Height of the liquid bridge
As	: Aspect ratio (=H/R)
K	: Dimensionless shielding parameter ($=\sigma\mu_0\omega R^2$)
μ	: Permeability of melt
$\vec{B}$	: external RMF
B_0	: Amplitude of RMF
B_r	: component of RMF in the radial direction
B_θ	: component of RMF in the azimuthal direction
B_x	: component of RMF in the x direction
B_y	: component of RMF in the y direction
Pr	: Prandtl number
Ta	: Taylor number
Re_ω	: Rotation magnetic Reynolds number
u^*	: Dimensionless velocity component in the x direction
v^*	: Dimensionless velocity component in the y direction
w^*	: Dimensionless velocity component in the z direction
ρ	: Density
η	: Dynamic viscosity
υ	: Kinematic viscosity
σ	: Electrical conductivity
κ	: Thermal diffusivity
ω	: Rotating angular frequency
λ	: Rotating frequency of RMF
$\vec{U}$	: Velocity vector
$\vec{E}$	: electric field
$\vec{j}$	: current density
ϕ	: Electrical potential
t^*	: Dimensionless time
P^*	: Dimensionless pressure
ϕ^*	: Dimensionless electrical potential
$\vec{U}^*$	: Dimensionless velocity vector
$\vec{f}^*_{rot}$	: Dimensionless Lorentz force
f_x^*	: Dimensionless component of the Lorentz force in the x direction
f_y^*	: Dimensionless component of the Lorentz force in the y direction

f_z^* : Dimensionless component of the Lorentz force in the z direction

References

[1] N. Armour and S. Dost, Cryst. Res. Technol. **3**, 45 (2010).
[2] V. V. Kalaev, J. Cryst. Growth **1**, 303 (2007).
[3] J. Priede, PhD thesis, University of Salaspils, Latvia (1993).
[4] T. J. Jaber, M. Z. Saghir, and A. Viviani, European Journal of Mechanics B-Fluids **2**, 28 (2008).
[5] L. Yao, and Z. Zeng, J. Cryst. Growth **1**, 316 (2011).
[6] L. Yao, Z. Zeng, and Y. Zhang, Cryst. Res. Technol. **8**, 47 (2012).
[7] L. Yao, Z. Zeng, and Y. Zhang, Heat Mass Transfer **12**, 48 (2012).
[8] L. Yao, Z. Zeng, and H. Mizuseki, Int. J. Therm. Sci. **12**, 49 (2010) .
[9] E. Dahlberg, Aktiebolaget Atomenergi, Sweden (1972).
[10] R. U. Barz, G. Gerbeth, and U. Wunderwald, J. Cryst. Growth **3-4**,180 (1997).
[11] M. P. Volz and K. Mazuruk, Int. J. Heat Mass Tran. **6**, 42 (1999).
[12] K. H. Spitzer, M. Dubke, and K. Schwerdtfeger, Metall. Mater. Trans. B **1**, 17 (1986).
[13] K. H. Spitzer, Prog. Cryst. Growth Ch. **1-4**, 38 (1999).
[14] Rafal Rakoczy and Stanislaw Masiuk, Chem. Eng. Sci. **11**, 66 (2011).
[15] R. J. Moreau, Magnetohydrodynamics, Springer Science & Business Media, France (2013) pp. 30-31.
[16] Y. Zhang, Z. Zeng, and L. Yao, Int. J. Appl. Electrom. **2**, 53 (2017).